Field information links permafrost carbon to physical vulnerabilities of thawing

Jennifer W. Harden,[1] Charles D. Koven,[2] Chien-Lu Ping,[3] Gustaf Hugelius,[4] A. David McGuire,[5] Phillip Camill,[6] Torre Jorgenson,[7] Peter Kuhry,[4] Gary J. Michaelson,[3] Jonathan A. O'Donnell,[8] Edward A. G. Schuur,[9] Charles Tarnocai,[10] Kristopher Johnson,[11] and Guido Grosse[12]

Received 9 April 2012; revised 29 June 2012; accepted 29 June 2012; published 7 August 2012.

[1] Deep soil profiles containing permafrost (Gelisols) were characterized for organic carbon (C) and total nitrogen (N) stocks to 3 m depths. Using the Community Climate System Model (CCSM4) we calculate cumulative distributions of active layer thickness (ALT) under current and future climates. The difference in cumulative ALT distributions over time was multiplied by C and N contents of soil horizons in Gelisol suborders to calculate newly thawed C and N. Thawing ranged from 147 PgC with 10 PgN by 2050 (representative concentration pathway RCP scenario 4.5) to 436 PgC with 29 PgN by 2100 (RCP 8.5). Organic horizons that thaw are vulnerable to combustion, and all horizon types are vulnerable to shifts in hydrology and decomposition. The rates and extent of such losses are unknown and can be further constrained by linking field and modelling approaches. These changes have the potential for strong additional loading to our atmosphere, water resources, and ecosystems.

Citation: Harden, J. W., et al. (2012), Field information links permafrost carbon to physical vulnerabilities of thawing, *Geophys. Res. Lett.*, *39*, L15704, doi:10.1029/2012GL051958.

1. Introduction

[2] CO_2 and CH_4 released from permafrost over the next century loom as an uncertain but potentially large feedback to global and regional warming. Northern soil C stocks and dynamics are sensitive to recent changes in soil temperatures [*Schuur et al.*, 2007], growing-season length [*Euskirchen et al.*, 2006], fire seasons [*Turetsky et al.*, 2011], nutrient availability [*Mack et al.*, 2004], and microbial processing of dissolved components [*Olefeldt and Roulet*, 2012], all of which are inter-related but highly heterogeneous across the landscape. Thus global models are challenged to resolve thaw-induced changes in trace-gas emissions in relation to three key attributes – C quantity, C form, and C environment – to evaluate the net effect of permafrost degradation. Soil N and soil C/N also play important roles in C cycle processes. Sparse data limit our ability to link process studies [*Natali et al.*, 2012] to larger scales and models [*Kimball et al.*, 2007].

[3] Permafrost-affected soils, or Gelisols [*Soil Survey Staff*, 1999] are mapped according to soil-forming processes. Turbels formed in the presence of cryoturbation (freeze-thaw mixing) of organic matter, with both gleyed and non-gleyed mineral materials. Histels have thick (>40 or 50 cm) organic soil horizons formed in the presence of a high or permafrost-induced water table. Orthels are permafrost soils that formed in the absence of cryoturbation or peat formation. Common to all Gelisols, freezing protects organic C from decomposition and combustion (Figure 1). Ground ice is key to processes of C stabilization and our accounting [*Grosse et al.*, 2011; *Jorgenson and Shur*, 2009] and greatly affects 1) the proportion of C in the active layer to permafrost [*Hugelius and Kuhry*, 2009] 2) the vulnerability of permafrost to disturbances [*Grosse et al.*, 2011], and 3) the contact time for organic substrates to interact with water and nutrients, which is key to mineral weathering and soil transformations [*Maher et al.*, 2009] that can stabilize C [*Torn et al.*, 1997]. C stabilization is also governed by long-term permafrost dynamics [*Sannel and Kuhry*, 2009], water saturation [*Zoltai and Vitt*, 1995], cryoturbation [*Bockheim*, 2007] sedimentation [*Schirrmeister et al.*, 2011] and other processes such as complexation with metals or mineral binding [*Lützow et al.*, 2006] (Figure 1a). Thawing is generally thought to promote C destabilization (Figures 1b and 1c), however, changes in hydrology and cyroturbation influence C stabilization as well, particularly in new accumulations of surface peat. Should future cooling occur, the return of permafrost and thinner active layers will likely promote restabilization of soil C.

[4] By the end of this century, processes of top-down thawing (active layer deepening; Figure 1b) and lateral thawing (thermokarst expansion) are hypothesized to remobilize comparable amounts of previously frozen soil C [*Hugelius et al.*, 2011]. While responses to both top-down and lateral progression of thaw are long-term goals for permafrost research, top-down thawing of permafrost is widespread and has been captured by a number of land models [e.g., *Koven et al.*,

[1]U.S. Geological Survey, Menlo Park, California, USA.
[2]Lawrence Berkeley National Laboratory, Berkeley, California, USA.
[3]Palmer Research Center, University of Alaska Fairbanks, Fairbanks, Alaska, USA.
[4]Department of Physical Geography and Quaternary Geology, Stockholm University, Stockholm, Sweden.
[5]Alaska Cooperative Fish and Wildlife Research Unit, University of Alaska Fairbanks, Fairbanks, Alaska, USA.
[6]Environmental Studies Program and Department of Earth and Oceanographic Science, Bowdoin College, Brunswick, Maine, USA.
[7]Alaska Ecoscience, Fairbanks, Alaska, USA.
[8]U.S. Geological Survey, Boulder, Colorado, USA.
[9]Department of Biology, University of Florida, Gainesville, Florida, USA.
[10]Agriculture and Agri-Food Canada, Ottawa, Ontario, Canada.
[11]USDA Forest Service, Newtown Square, Pennsylvania, USA.
[12]Geophysical Institute, University of Alaska Fairbanks, Fairbanks, Alaska, USA.

Corresponding author: J. W. Harden, U.S. Geological Survey, 345 Middlefield Rd., Menlo Park, CA 94025, USA. (jharden@usgs.gov)

0094-8276/12/2012GL051958

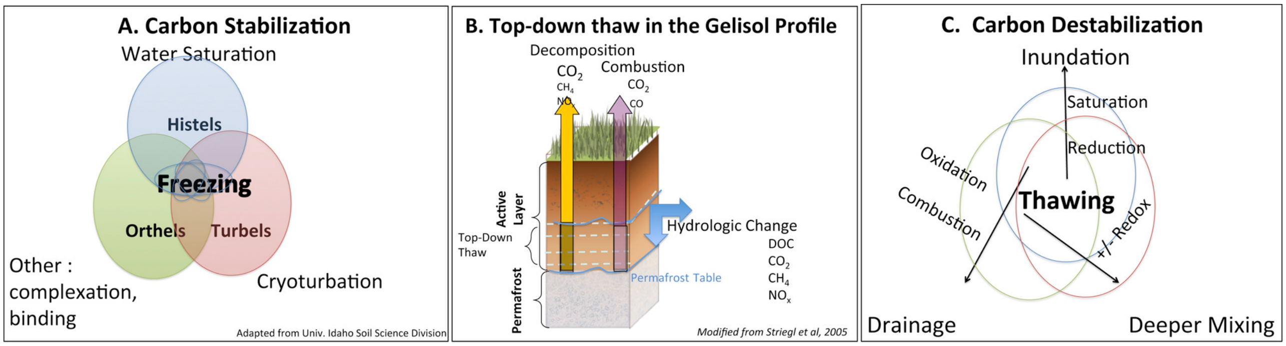

Figure 1. Permafrost soils and processes affecting carbon: (A) The 3 suborders (ovals) of Gelisols, or permafrost soils, and the processes that dominate their formation and C stabilization. Other processes of C stabilization are ice aggradation, important in all but very dry soils; active layer thinning, which promotes ice aggradation and freezing; and syngenetic accumulation of ice with organic and mineral materials as landforms accrete upward. For Histels, syngenesis of ice and peat occurs; for Orthels and Turbels, syngenesis of ice with mineral or organo-mineral soil occurs. (B) Top-down thaw and impacts on C losses (arrows) from the soil profile; modified from [*Striegl et al.*, 2005]. (C) Potential C destabilization upon thawing, showing shifts (arrows) in the processes involved in classification of suborders (ovals as in panel B). Processes of C destabilization (arrows) align along pathways dictated by water and mixing. Over long-term histories, both B and C occurred in response to climate and ecosystem processes resulting in soil profiles we see today. For future scenarios represented by current models, processes in part C are assumed to outpace B owing to continued warming, but hydrologic changes and landform accretion/collapse are not yet captured by models.

2011; *Lawrence et al.*, 2008]. Meanwhile, permafrost C inventories [*Tarnocai et al.*, 2009; *Ping et al.*, 2008a] have not yet established detailed vertical distributions for soil horizons and their C stocks that are suitable for use by large scale land models and have only been determined thus far at local/regional scales [e.g., *Hugelius et al.*, 2011]. Representing the effects of vertical thaw on soil C dynamics would be greatly advanced by linking to a more detailed characterization of the depth and horizon distributions of soil C and N. To this end, we have linked field- and lab-based soil information to models of top-down permafrost thawing in order to elucidate specific vulnerabilities of soil C to thawing. Field information on soil horizons such as organic, mineral, gleyed, cryoturbated allowed us to explore means and variations in depths, densities, and thicknesses for each of 3 gelisol suborders. Spatial maps of the suborders allowed us to link such means to potential exposures to specific vulnerabilities based on the depth and type of soil horizon affected by thawing.

2. Approach

2.1. Calculation of C and N Depth Distributions by Characteristic Horizon Types

[5] For each soil pedon, we determined C and N densities, C and N stocks, and C/N at 5-cm depth increments and attributed each increment to one of six characteristic horizon types (Noncryoturbated-Nongleyed, Noncryoturbated-Gleyed, Cryoturbated-Nongleyed, Cryoturbated-Gleyed, Fibrous Organic, and Amorphous Organic). For each of the three gelisol suborders, we then calculated means and standard deviations for each horizon type occurring within each depth increment. Lab errors for C content and bulk density are accounted for in spatial replication of profiles (equations (1) and (2) in the auxiliary material).[1] Analysis of variance (ANOVA) was used to examine differences among horizons in C and N densities, C and N stocks, and C/N (see auxiliary material).

2.2. Thawing of Permafrost

[6] We estimate the statistical distribution of freeze/thaw as a function of depth for permafrost soils by calculating the cumulative distribution of active layer thickness (ALT) for all permafrost gridcells of the CCSM4 for each of 3 time periods: current (yr 2005–2014), mid-century (2045–2054), and end-of-century (2090–2099) using RCP4.5 and RCP8.5 which refer to stabilized radiative forcings at levels of 4.5 and 8.5 W/m^2 by 2100. Model output for current periods are compared to measurements of ALT (see Figure 3a) to evaluate model performance. The CCSM4 includes soil parameterizations for organic and mineral substrates and their thermal and hydrologic properties at multiple depths to >30 m [*Lawrence et al.*, 2011]. However, we limit our analysis to 3 m depths where our soil data were most robust. Once thawed, the differences between current and future ALT distributions were then used to quantify the amounts of C and N in various horizon types that were subjected to future thaw. This was accomplished by establishing separate cumulative ALT distributions for each suborder, which were then combined with depth profiles of permafrost carbon attributed to horizon type:

$$Cv_{hor} = \sum_{suborder} A_{suborder} \int C_{hor,suborder}(z) \Delta F_{suborder}(z) dz \qquad (1)$$

where: Cv_{hor} is the C vulnerable to changes in ALT of a given horizon type; *hor* is the horizon type (two organic, four mineral); *suborder* is the suborder (Histel, Orthel, Turbel); $A_{suborder}$ is the total area covered by soils of the suborder; $C_{hor,suborder}(z)$ is the C density for a given horizon type and suborder at depth; (z) is the change in frozen fraction for suborder at depth z.; $\Delta F_{suborder}(z)$ therefore is based on the cumulative ALT distributions from each time period.

[1]Auxiliary materials are available in the HTML. doi:10.1029/2012GL051958.

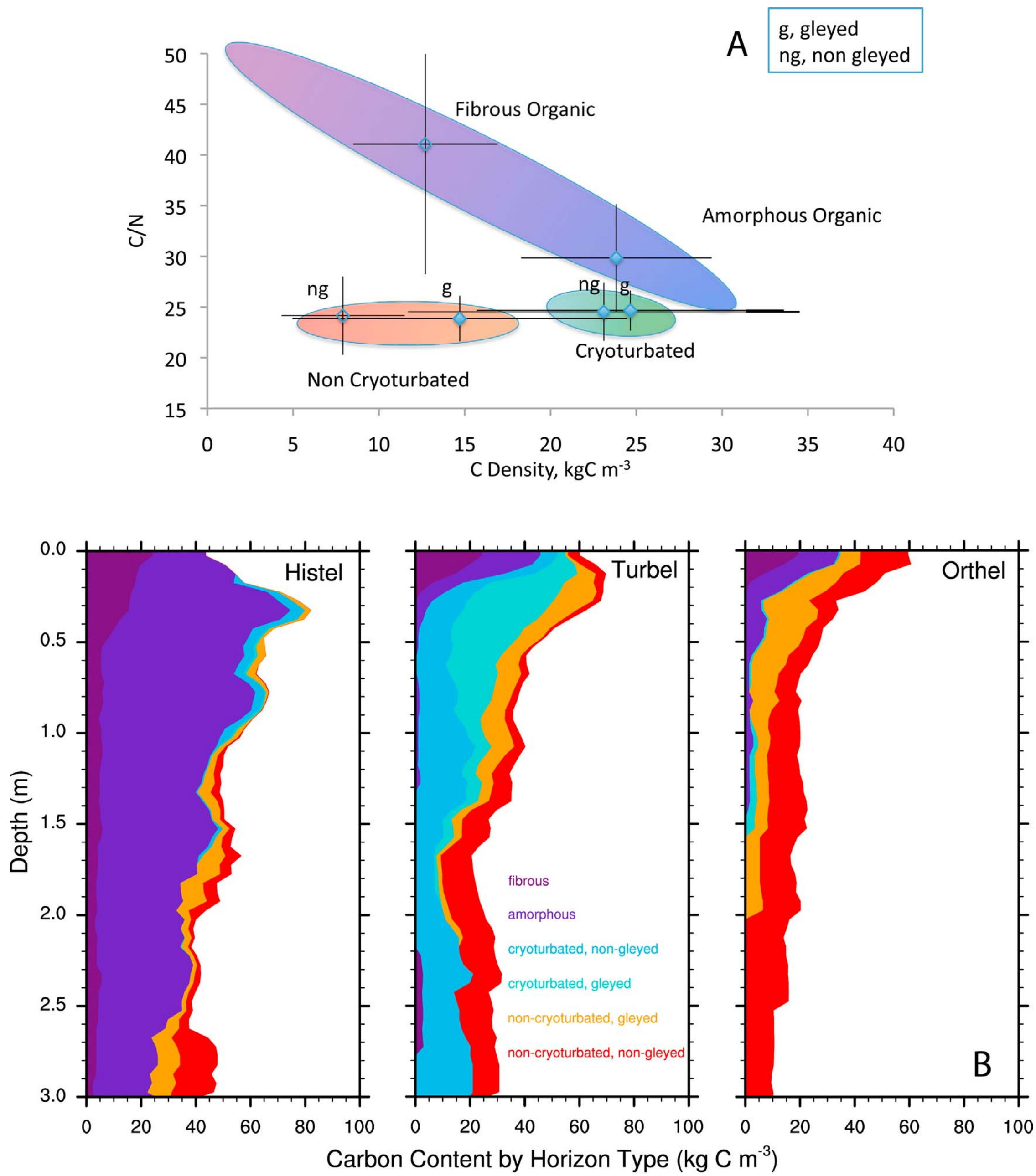

Figure 2. (a) The relationship between C/N ratio and C density in kgC/m^3 across soil horizons and the carbon - depth distributions of soil horizons in (b) Histels, (c) Turbels and (d) Orthels. Organic horizons (circled) with >10% C include fibrous and amorphous forms; Cryoturbated horizons (circled) include nongleyed (NG) and gleyed (G) oxidative states. Mean and standard deviations shown in A. Noncryoturbated horizons (circled) include gleyed and nongleyed states. Samples with % N <0.1 were omitted from this analysis (see Table S1). Colors in Figure 2a are matched to those in Figures 2b–2d.

[7] Uncertainty was evaluated by including end-member estimates for both thawing and carbon stock estimates for each of the suborders (for more information, see auxiliary material).

3. Findings

3.1. Carbon and Nitrogen in Permafrost Soils

[8] Organic C to 3 m varies according to suborders, ranging from Histels (best estimate 160 kgC/m^2), Turbels (110) to Orthels (71) with total N stocks ranging from Histels (6.9 kgN/m^2) Orthels (4.6) and Turbels (7.5) to 3 m depths. Uncertainties for these stocks are sensitive to several assumptions and could range from 10 to 100 kgC and <1 to 226 kgN depending on methods for propagating errors (auxiliary material). Types of soil horizons, which are recognized and sampled in the field, show consistent and significant differences in C and N among suborders (ANOVA; P < 0.05; see auxiliary material for details). Organic horizons have higher C/N than mineral horizons (Figure 2a; P < 0.001). Histels are characterized by fibrous and amorphous organic horizons with high C densities and wide ranges in

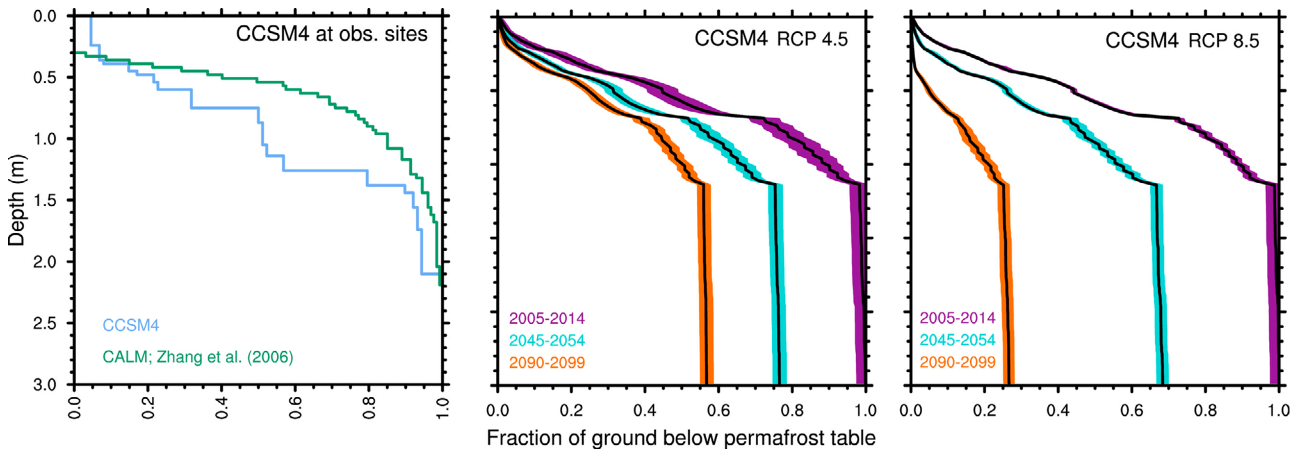

Figure 3. (a) Comparison of cumulative active layer thickness (ALT) distributions from CCSM4 model and the observations of the CALM network [*Brown et al.*, 2000] and the dataset of *Zhang et al.* [2006]. Modeled ALT values are sampled at each gridcell corresponding to a site from the observation networks. Cumulative ALT distributions from all permafrost-containing gridcells of the CCSM4 model for period 2005–2014, 2045–2054, and 2090–2099 using climate scenarios (b) RCP4.5 and (c) RCP8.5. Shaded area represents 1SD model spread within the ensemble for each scenario.

C/N values (with higher C/N in fibrous horizons; ANOVA, $P < 0.05$; Figure 2a), reflecting long-term net accumulation of plant substrates with wide ranges in N contents and decomposition histories. C density is highest in amorphous organic horizons and cryoturbated horizons (ANOVA $p < 0.05$). Large quantities of carbon in intermediate depths of Turbels reflect advection of organic matter into mineral substrates by cryoturbation (Figure 2c) [*Koven et al.*, 2009]. Gleyed cryoturbated horizons indicate proximity to the "permafrost table" (Figure 2c; see also Figure 3) where seasonal water is typically perched long enough to promote anoxic conditions [*Bockheim*, 1980, 2007; *Ping et al.*, 2008b]. The %C and N in gleyed mineral soil horizons is higher than in non-gleyed horizons (ANOVA; $P < 0.05$) which reflects accumulation of organic matter near the permafrost table [*Ping et al.*, 2008b]. The mechanisms of C stabilization are captured by the suborder classification in that Histels reflect saturation and subsequent freezing of organic soil horizons (Figure 2b); Turbels reflect advection of organic matter into deeper parts of the active layer that subsequently freezes into permafrost (Figure 2c); and Orthels reflect a combination of processes including stabilization by freezing into the permafrost (Figure 2d).

3.2. Thawing

[9] The cumulative ALT distributions calculated by CCSM4 for current and future climates (Figures 3b and 3c), show that under the current climate, 45% of permafrost soils have ALT $\leq$ 1 m. About 25% and 5% of permafrost soils will have ALT $\leq$ 1 m by 2100 under RCP4.5 and RCP8.5, respectively. Similarly, the model projects that only 57% and 26% of area of permafrost soils will still contain permafrost in the top 3 m by the end of the century under the RCP4.5 and RCP8.5 scenarios, respectively.

[10] Model output from gridcells that contain measurements of ALT (Figure 3a) shows a tendency of CCSM4 to overestimate ALT under current climates (see Figure 3a). This is partly due to biases, such as excessive snowfall in the atmospheric model and its associated insulation [*Lawrence et al.*, 2012], but model-data bias also indicates variables and processes presently not accounted for in the model, such as variable ground ice content, lateral heat flux, and feedbacks between fire and thaw. The effect of these biases on our calculations are complex—for example, overestimation of ALT suggests an underestimate of the fraction of C that is initially in permafrost and therefore available for thaw. For modeling the sensitivity of permafrost to warming, the atmospheric biases and lack of representing massive ice suggests the model overestimates this sensitivity, while the lack of lateral or bottom-up thaw and fire feedbacks may indicate the model underestimates this sensitivity.

3.3. Carbon and Nitrogen Sensitivities to Thawing

[11] Our model results (Table 1) project that permafrost layers within the top 3 m of permafrost-affected soils contain 135 to 881 Pg of C today (best estimate 474 Pg), with another 122 to 1012 Pg stored in seasonally (surface) or perennially (talik) thawed soils. Permafrost layers also contain 31 to 102 Pg of N (best estimate 66). These ranges include variations in both ALT and depth distributions of C and N. Over the next century, under the moderate warming scenario (RCP4.5), we estimate that 61 to 399 Pg (best estimate 214 Pg) of permafrost C will thaw, with concomitant thawing of 16 Pg of N. Under the high RCP8.5 warming scenario, 108–706 Pg (best estimate 379 Pg) of permafrost C, and 29 Pg of N, may thaw by 2100 (Table 1). These estimates are constrained to the uppermost 3 m and do not include deeper soils and sediments such as deltaic deposits or Yedoma (Pleistocene deposits rich in ice and carbon) that may also be subjected to thawing and contain large stocks of C.

[12] Once thawed, several pathways for C release are feasible. All newly thawed carbon is likely to experience enhanced decomposition and hydrologic shifts such as leaching, ponding, or draining. Depending on whether hydrological shifts favor drainage or ponding (Figure S2), which is heterogeneous [*Turetsky et al.*, 2005] and difficult to predict, enhanced oxidation or reduction will determine the reaction pathway and fate of the thawing C and N. Organic horizons will become susceptible to combustion

Table 1. Organic C and Total N in Frozen and Thawed Soils According to Model Forecasting by CCLM4[a]

	Present Day Total C[b]			Present Day Permafrost C[b]			C Thawed by yr 2050 rcp4.5[b,c,d]			C Thawed by 2050 rcp8.5[b,c,d]	C Thawed by 2100 rcp4.5[b,c,d]	C Thawed by 2100 rcp8.5[b,c,d]		
	Best Estimate	Min	Max	Best Estimate	Min	Max	Best Estimate	Min	Max	Best Estimate	Best Estimate	Best Estimate	Min	Max
Key Vulnerabilities of O Horizons Upon Thawing: Decomposition and Combustion														
O horizons	**251**	38	613	**99**	19	232	**27**	5	64	**38**	**45**	**80**	16	187
Key Vulnerabilities of Gleyed Horizons Upon Thawing: Decomposition and Hydrologic Change														
Gleyed horizons	**280**	4	776	**83**	0	291	**26**	0	86	**36**	**40**	**71**	0	244
Key Vulnerabilities of Cryoturbated Horizons Upon Thawing: Decomposition and Hydrologic Change														
Cryoturbated horizons	**408**	17	979	**202**	11	482	**55**	3	132	**77**	**92**	**162**	8	389
All horizon Carbon[e]	**1060**	223	2159	**548**	134	1063	**147**	35	287	**208**	**246**	**436**	105	851
All horizon Nitrogen	**67**	28	106	**37**	18	56	**10**	5	15	**14**	**17**	**29**	14	44

[a]Units in Petagrams C. Uncertainties show and minimum and maximum values as in the auxiliary material.
[b]Includes propagated errors for variance in measured profile-based carbon inventories; measurement uncertainty of bulk density.
[c]Includes uncertainty of present-day models of frozen/unfrozen areas and their relationship to depth using probability distributions; also includes uncertainty related to models for future thawing and variations in the shape of the thaw curve . See auxiliary material.
[d]Recognized unmeasured uncertainty related to C vulnerability unrelated to thawing such as fire, dissolved export, and other thawing mechanisms such as lateral thermokarst.
[e]All horizon carbon and nitrogen include also non-cryoturbated and non-gleyed horizons.

under enhanced post-thaw drainage, thus as much as 16 to 187 Pg C (best estimate 80 Pg C for RCP 8.5; compare to 33 Pg for Histels according to *Wisser et al.* [2011]) could be newly subjected to combustion by wildfire, potentially as a more rapid emission pathway than through decomposition (Table 1).

[13] The stocks of vulnerable C listed in Table 1 should not be seen as the total amount of C that will be released due to thaw. Incubation and substrate studies [e.g., *Dioumaeva et al.*, 2002; *Dutta et al.*, 2006; *Schimel and Mikan*, 2005] suggest that large fractions of labile C exist in arctic soils, including permafrost layers. Yet even in long (~1-year) incubations [*Dutta et al.*, 2006], less than 3% of initial C was lost to decomposition at room temperature in the absence of new substrates or nutrients. Little is known about whether such decomposition rates are fractionally proportional over longer time-frames (>1-year). Even less is known about field conditions for deep soil decomposition and deep permafrost, although some recent field studies indicate enhanced decomposition occurs post-thaw [*Nowinski et al.*, 2010; *O'Donnell et al.*, 2009, 2012; *Schuur et al.*, 2007] and that microbial communities are viable even after long periods of being frozen [*Mackelprang et al.*, 2011]. Cold temperatures (even during the thaw season), limits to oxygen and nutrient availability, stabilization processes such as mineral binding or cryoturbation, and flowpaths for dissolved organic matter play important roles in determining the rate of soil C emissions and their contribution to feedbacks through nutrient cycling. Furthermore, the association of incubation- and water extraction-based studies of dissolved C fractions [*Michaelson and Ping*, 2003] have only been weakly associated to horizon forms as described and sampled in pedon studies. While more and better spatial coverage of complete soil profiles, particularly in undersampled regions such as Siberia, will continue to improve estimates of amounts and forms of carbon in soils, measurements that link moisture-redox-gas and dissolved C fluxes to specific soil horizons will enable us to explicitly link the spatial information of soil profiles and horizons to C transfer functions established experimentally.

[14] Reported uncertainties (Table 1) are based on 1 standard deviation of C densities from the pedon-level observations; higher estimates could result from deeper soil materials and lower estimates could result from rocky or ice-rich substrates. In addition, substantial uncertainties exist that are more difficult to quantify. One of these is the CCSM4 overestimate of ALT due to excessive snow (Figure 3a; see also auxiliary material). It is not clear, however, whether we have underestimated future thawing by propagating this bias through the future climate scenarios because thaw is defined as the difference between future and current ALT. Our approach neglects possible spatial covaration between soil C and ALT, which may lead to errors in thawed carbon if, for example, C profiles differ greatly between (a) warm and vulnerable permafrost soils vs. cold and stable permafrost, or (b) between Histels and mineral soils existing within what the model treats as a single grid-cell; these issues reinforce the need for (a) more observations of continental and southerly permafrost soils, and (b) explicit differentiation within land surface models of sub-gridscale difference in soil types. Issues that may reduce these estimates involve how we treat deep observations (we assumed missing data here but rock or pure ice could indicate near-zero values for %C) and our ability to represent high-ice, low carbon soils in our sampling. Moreover, our model does not capture abrupt or spatially heterogeneous impacts on soil C and N such as due to thermokarst formation or changes in hydrology, talik, fire severity, or vegetation community, and also does not take into account the important role of thermokarst lakes in releasing very deep permafrost C. Yet the timing and duration of such processes likely profoundly influence the trends captured by this top-down thawing approach, potentially resulting in even greater releases of C and N.

[15] **Acknowledgments.** This collaboration was supported by the Vulnerability of Permafrost Carbon Research Coordination Network and its numerous funding agencies. We also acknowledge USGS, DOE/BER DE-AC02-05CH11231 and Swedish Research Council. We gratefully acknowledge helpful reviews by Julie Jastrow and Kristen Manies.

[16] The Editor thanks Julie Jastrow and an anonymous reviewer for assisting in the evaluation of this paper.

References

Bockheim, J. G. (1980), Solution and use of chronofunctions in studying soil development, *Geoderma*, *24*, 71–85, doi:10.1016/0016-7061(80)90035-X.

Bockheim, J. G. (2007), Importance of cryoturbation in redistributing organic carbon in permafrost-affected soils, *Soil Sci. Soc. Am. J.*, *71*(4), 1335–1342, doi:10.2136/sssaj2006.0414N.

Brown, J., K. Hinkel, and F. Nelson (2000), The Circumpolar Active Layer Monitoring (CALM) program: Research designs and initial results, *Polar Geogr.*, *24*, 165–258.

Dioumaeva, I., S. Trumbore, E. A. G. Schuur, M. L. Goulden, M. Litvak, and A. I. Hirsch (2002), Decomposition of peat from upland boreal forest: Temperature dependence and sources of respired carbon, *J. Geophys. Res.*, *107*(D3), 8222, doi:10.1029/2001JD000848.

Dutta, K., E. A. G. Schuur, J. C. Neff, and S. A. Zimov (2006), Potential carbon release from permafrost soils of northeastern Siberia, *Global Change Biol.*, *12*(12), 2336–2351, doi:10.1111/j.1365-2486.2006.01259.x.

Euskirchen, E. S., et al. (2006), Importance of recent shifts in soil thermal dynamics on growing season length, productivity, and carbon sequestration in terrestrial high-latitude ecosystems, *Global Change Biol.*, *12*(4), 731–750, doi:10.1111/j.1365-2486.2006.01113.x.

Grosse, G., et al. (2011), Vulnerability of high-latitude soil organic carbon in North America to disturbance, *J. Geophys. Res.*, *116*, G00K06, doi:10.1029/2010JG001507.

Hugelius, G., and P. Kuhry (2009), Landscape partitioning and environmental gradient analyses of soil organic carbon in a permafrost environment, *Global Biogeochem. Cycles*, *23*, GB3006, doi:10.1029/2008GB003419.

Hugelius, G., T. Virtanen, D. Kaverin, A. Pastukhov, F. Rivkin, S. Marchenko, V. Romanovsky, and P. Kuhry (2011), High-resolution mapping of ecosystem carbon storage and potential effects of permafrost thaw in periglacial terrain, European Russian Arctic, *J. Geophys. Res.*, *116*, G03024, doi:10.1029/2010JG001606.

Jorgenson, M. T., and Y. L. Shur (2009), Permafrost, in *The Oxford Companion to Global Change*, edited by A. Goudie and D. Cuff, pp. 540–547, Oxford Univ. Press, Oxford, U. K.

Kimball, J. S., et al. (2007), Climate driven increases in boreal and Arctic vegetation productivity: Evidence of decreasing stability of the northern high latitude terrestrial carbon reservoir, *Earth Interact.*, *11*(4), 1–30, doi:10.1175/EI180.1.

Koven, C., P. Friedlingstein, P. Ciais, D. Khvorostyanov, G. Krinner, and C. Tarnocai (2009), On the formation of high-latitude soil carbon stocks: Effects of cryoturbation and insulation by organic matter in a land surface model, *Geophys. Res. Lett.*, *36*, L21501, doi:10.1029/2009GL040150.

Koven, C. D., B. Ringeval, P. Friedlingstein, P. Ciais, P. Cadule, D. Khvorostyanov, G. Krinner, and C. Tarnocai (2011), Permafrost carbon-climate feedbacks accelerate global warming, *Proc. Natl. Acad. Sci. U. S. A.*, *108*(36), 14,769–14,774, doi:10.1073/pnas.1103910108.

Lawrence, D. M., A. G. Slater, V. E. Romanovsky, and D. J. Nicolsky (2008), Sensitivity of a model projection of near-surface permafrost degradation to soil column depth and representation of soil organic matter, *J. Geophys. Res.*, *113*, F02011, doi:10.1029/2007JF000883.

Lawrence, D., et al. (2011), Parameterization improvements and functional and structural advances in version 4 of the Community Land Model, *J. Adv. Model. Earth Syst.*, *3*, M03001, doi:10.1029/2011MS000045.

Lawrence, D. M., A. G. Slater, and S. C. Swenson (2012), Simulation of present-day and future permafrost and seasonally frozen ground conditions in CCSM4, *J. Clim.*, *25*, 2207–2225, doi:10.1175/JCLI-D-11-00334.1.

Lützow, M. V., I. Kögel-Knabner, K. Ekschmitt, E. Matzner, G. Guggenberger, B. Marschner, and H. Flessa (2006), Stabilization of organic matter in temperate soils: Mechanisms and their relevance under different soil conditions—A review, *Eur. J. Soil Sci.*, *57*(4), 426–445, doi:10.1111/j.1365-2389.2006.00809.x.

Mack, M. C., E. A. G. Schuur, M. S. Bret-Harte, G. R. Shaver, and F. S. I. Chapin (2004), Carbon storage in arctic tundra reduced by long-term nutrient fertilization, *Nature*, *431*, 440–443, doi:10.1038/nature02887.

Mackelprang, R., M. P. Waldrop, K. M. DeAngelis, M. M. David, K. L. Chavarria, S. J. Blazewicz, E. M. Rubin, and J. K. Jansson (2011), Deep metagenome sequencing illuminates permafrost response to thaw, *Nature*, *480*(7377), 368, doi:10.1038/nature10576.

Maher, K., C. I. Steefel, A. F. White, and D. A. Stonestrom (2009), The role of reaction affinity and secondary minerals in regulating chemical weathering rates at the Santa Cruz Soil Chronosequence, California, *Geochim. Cosmochim. Acta*, *73*(10), 2804–2831, doi:10.1016/j.gca.2009.01.030.

Michaelson, G. J., and C. L. Ping (2003), Soil organic carbon and CO_2 respiration at subzero temperature in soils of Arctic Alaska, *J. Geophys. Res.*, *108*(D2), 8164, doi:10.1029/2001JD000920.

Natali, S. M., E. A. G. Schuur, and R. L. Rubin (2012), Increased plant productivity in Alaskan tundra as a results of experimental warming of soil and permafrost, *J. Ecol.*, *100*(2), 488–498, doi:10.1111/j.1365-2745.2011.01925.x.

Nowinski, N. S., L. Taneva, S. E. Trumbore, and J. M. Welker (2010), Decomposition of old organic matter as a result of deeper active layers in a snow depth manipulation experiment, *Oecologia*, *163*, 785–792, doi:10.1007/s00442-009-1556-x.

O'Donnell, J. A., M. R. Turetsky, J. W. Harden, K. L. Manies, L. E. Pruett, and J. C. Neff (2009), Interactive effects of fire, soil climate, and vegetation in CO_2 fluxes in an upland black spruce forest and peatland in interior Alaska, *Ecosystems*, *12*(1), 52–72.

O'Donnell, J. A., M. T. Jorgenson, J. W. Harden, A. D. McGuire, M. Z. Kanevskiy, and K. P. Wickland (2012), The effects of permafrost thaw on soil hydrologic, thermal and carbon dynamics in an Alaskan peatland, *Ecosystems*, *15*, 213–229, doi:10.1007/s10021-011-9504-0.

Olefeldt, D., and N. T. Roulet (2012), Effects of permafrost and hydrology on the composition and transport of dissolved organic carbon in a subarctic peatland complex, *J. Geophys. Res.*, *117*, G01005, doi:10.1029/2011JG001819.

Ping, C.-L., G. J. Michaelson, M. T. Jorgenson, J. M. Kimble, H. Epstein, V. E. Romanovsky, and D. A. Walker (2008a), High stocks of soil organic carbon in the North American Arctic region, *Nat. Geosci.*, *1*, 615–619, doi:10.1038/ngeo284

Ping, C.-L., G. J. Michaelson, J. M. Kimble, V. E. Romanovsky, Y. L. Shur, D. K. Swanson, and D. A. Walker (2008b), Cryogenesis and soil formation along a bioclimate gradient in Arctic North America, *J. Geophys. Res.*, *113*, G03S12, doi:10.1029/2008JG000744.

Sannel, A. B. K., and P. Kuhry (2009), Holocene peat growth and decay dynamics in sub-arctic peat plateaus, west-central Canada, *Boreas*, *38*(1), 13–24, doi:10.1111/j.1502-3885.2008.00048.x.

Schimel, J. P., and C. Mikan (2005), Changing microbial substrate use in Arctic tundra soils through a freeze-thaw cycle, *Soil Biol. Biochem.*, *37*(8), 1411–1418, doi:10.1016/j.soilbio.2004.12.011.

Schirrmeister, L., G. Grosse, S. Wetterich, P. P. Overduin, J. Strauss, E. A. G. Schuur, and H.-W. Hubberten (2011), Fossil organic matter characteristics in permafrost deposits of the northeast Siberian Arctic, *J. Geophys. Res.*, *116*, G00M02, doi:10.1029/2011JG001647.

Schuur, E. A. G., J. G. Vogel, K. Dutta, K. G. Crummer, and H. Lee (2007), The Contribution of old carbon to respiration from Arctic tundra following permafrost thaw, *Eos Trans. AGU*, *88*(52), Fall Meet. Suppl., Abstract B21C-07.

Soil Survey Staff (1999), *Soil Taxonomy: A Basic System of Soil Classification for Making and Interpreting Soil Surveys*, *Agric. Handb.*, vol. 436, U.S. Gov. Print. Off., Washington, D. C.

Striegl, R. G., G. R. Aiken, M. M. Dornblaser, P. A. Raymond, and K. P. Wickland (2005), A decrease in discharge-normalized DOC export by the Yukon River during summer through autumn, *Geophys. Res. Lett.*, *32*, L21413, doi:10.1029/2005GL024413.

Tarnocai, C., J. G. Canadell, E. A. G. Schuur, P. Kuhry, G. Mazhitova, and S. Zimov (2009), Soil organic carbon pools in the northern circumpolar permafrost region, *Global Biogeochem. Cycles*, *23*, GB2023, doi:10.1029/2008GB003327.

Torn, M. S., S. E. Trumbore, O. A. Chadwick, P. M. Vitousek, and D. M. Hendricks (1997), Mineral control of soil organic carbon storage and turnover, *Nature*, *389*, 170–173, doi:10.1038/38260.

Turetsky, M. R., M. C. Mack, J. W. Harden, and K. L. Manies (2005), Spatial patterning of soil carbon storage across boreal landscapes, in *Ecosystem Function in Heterogeneous Landscapes*, edited by G. M. Lovett et al., pp. 229–255, Springer, New York, doi:10.1007/0-387-24091-8_12.

Turetsky, M. R., E. S. Kane, J. W. Harden, R. D. Ottmar, K. L. Manies, E. Hoy, and E. S. Kasichke (2011), Recent acceleration of biomass burning and carbon losses in Alaskan forests and peatlands, *Nat. Geosci.*, *4*, 27–31, doi:10.1038/ngeo1027.

Wisser, D., S. Marchenko, J. Talbot, C. Treat, and S. Frolking (2011), Soil temperature response to 21st century global warming: The role of and some implications for peat carbon in thawing permafrost soils in North America, *Earth Syst. Dyn.*, *2*, 121–138, doi:10.5194/esd-2-121-2011.

Zhang, Y., W. Chen, and D. W. Riseborough (2006), Temporal and spatial changes of permafrost in Canada since the end of the Little Ice Age, *J. Geophys. Res.*, *111*, D22103, doi:10.1029/2006JD007284.

Zoltai, S. C., and D. H. Vitt (1995), Canadian wetlands: Environmental gradients and classification, *Plant. Ecol.*, *118*(1–2), 131–137, doi:10.1007/BF00045195.